Statistical model of nuclear multifragmentation

A. R. DeAngelis and A. Z. Mekjian
Department of Physics and Astronomy, Rutgers University, New Brunswick, New Jersey 08901
(Received 22 April 1988; revised manuscript received 23 March 1989)

We present a statistical approach to the problem of multifragmentation in heavy-ion collisions. We begin with a generalized Sakur-Tetrode expression for the entropy. Through it we find expressions for the configuration weight functions. Fluctuations in the configurations are shown to be Poisson-like. Fragmentation yields are calculated by minimizing the total information subject to conservation of energy and baryon number. We work within the framework of a liquid-gas phase transition, and include a study of the effects of the nuclear surface (including a surface curvature correction), the Coulomb energy, and the internal excited states of the drop. Coulomb effects are investigated using both a simple $A^{5/3}$ dependence (as in the liquid-drop model) and a more complete expression which includes the presence of the surrounding vapor. We adopt a virial expansion for the equation of state and have found an analytic solution for the coexistence curve in infinite, uncharged matter. The case of charged, finite matter is also discussed. By identifying the clusters with the nuclei which are detected experimentally we can calculate fragment yields over a range of temperatures. We do so for a representative case and discuss the results.

I. INTRODUCTION

Heavy-ion collisions offer the possibility of studying new phases of nuclei. Two new phases are of current interest. One phase is the low density, moderate temperature region near a liquid-gas phase transition. Medium energy heavy-ion collisions, in which the excitation energy per nucleon is near the separation energy, are a useful probe of this region. The other phase is the high-density, high temperature region around a quark-gluon plasma-hadron phase transition. Ultrarelativistic heavy-ion collisions are being used to study such a transition. In both cases one can study the transition by looking at the distribution of products in composition and momentum space. This paper is concerned with the liquid-gas transition, and we will be concerned primarily with the distribution in composition of the final products.

Recently, considerable interest has centered around the idea of nuclear multifragmentation.[1–8] Properties of nuclear drops in the presence of a vapor of nucleons are also of interest in astrophysics.[9,10] For systems whose temperatures are far below the critical point one has the Weisskopf evaporation picture, recently extended by Friedman and Lynch.[11] For temperatures above the critical point one has a gas of nucleons plus recombined clusters.[12–15]

Two key papers on multifragmentation came from a Purdue-Fermilab collaboration,[16] which discovered a power law falloff in the distribution in composition of the observed species as a function of mass number. This power law falloff had been predicted by a droplet model theory of condensation developed by Fisher.[17] In Fisher's model the droplet mass distribution near a critical point fell as $A^{-\tau}$ where τ is the critical exponent. This similarity has prompted much activity in models of heavy-ion collisions based on phase transitions.

In the transition region between liquid evaporation and gas recombination, the nuclear system has a critical point. Near the critical point the droplet yield distribution should show the phenomenon of critical opalescence, and many nuclear fragments of varying sizes should be present in the distribution in composition. Fluctuations will also be large in this region of temperature. A theory which bridges the gap between the results of the evaporation model and the gas recombination model is of importance for medium energy heavy-ion collision. Several approaches to this problem are now being developed, including thermodynamic models.

If one assumes that the colliding ions form a thermalized vapor of nucleons, then one can apply a statistical analysis to describe the composition of the system. In this paper we discuss nuclear multifragmentation within the framework of a grand canonical model. We then find the distribution of nucleons which maximizes the entropy as it is given by a generalized Sackur-Tetrode law including internal excitations of the clusters, and show that fluctuations around this most probable distribution are given by a Poisson-type expression. Our model includes volume, surface, and surface curvature correction terms. In addition we have calculated the Coulomb energy in a mean-field which includes the effects of the vapor. We discuss the form for each of these terms. To relate density and temperature we start with a virial expansion for the equation of state. Applying the Gibbs criteria for phases in equilibrium allows us to find the coexistence curves. It turns out that at the critical temperature these curves are identical to those in a ferromagnetic transition.

Conservation of energy and mass number are incorporated through the method of Lagrange multipliers. Using our constraints and the requirement that the entropy be maximized we have calculated the expected yields in a heavy-ion collision as a function of fragment mass number. Our calculations were done with different forms for the Coulomb energy so that we could study the im-

portance of the Coulomb term in determining fragment yields. The results show the importance of including the vapor and the effects of temperature on the yields.

II. MAXIMUM ENTROPY APPROACH

We begin with a gas of A_0 nucleons and ask how it will partition itself into clusters. These clusters we shall associate with bound nuclei. Figure 1 is a schematic illustration of this process. From within a gas of radius R_g^0 and charge density $\xi_g(z)$ forms a cluster of nucleons of radius R_l and charge density $\xi_l(z)$. This cluster is a liquid drop immersed in a vapor. The gas density does not change, so that the radius of the system shrinks to R_g. Although the figure shows only one cluster forming, we assume the process of clustering occurs simultaneously throughout the gas. This allows us to assign the same temperature to every cluster. Eventually all the nucleons in the gas are contained in clusters from size one to A_0.

Whether or not clustering is actually a prompt process is an open problem which we do not consider here. In this paper we restrict ourselves to the question of which size clusters tend to form. We shall try to answer it by identifying the most probable of all the multitude of configurations into which the gas could cluster. This we can accomplish by maximizing the entropy subject to conservation of baryon number, charge, and energy. (In this paper we will assume $Z = A/2$ so that conservation of charge and baryon number are equivalent.) The answer will give us the relative yield of nuclei produced in heavy-ion collisions. By repeating the calculation over a range of temperatures and by using different forms for the energy we hope to unravel some of the physics involved in nuclear multifragmentation.

We begin with the entropy as given by the Sackur-Tetrode expression,[18] which we have generalized to include internal excitations of the clusters. The generalized form is

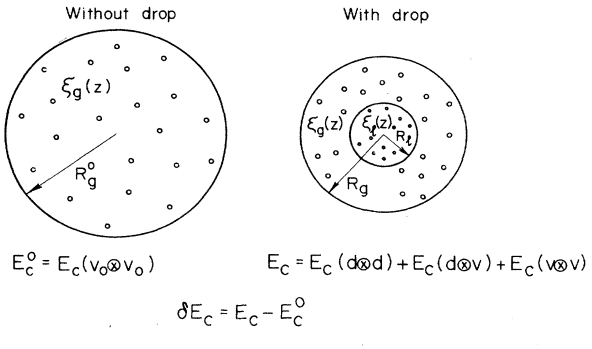

FIG. 1. Cluster formation in a vapor of nucleons. (a) shows a gas of nucleons with no clusters. In (b) a cluster of nucleons has coalesced into a liquid drop. When the cluster forms, the average density of the system increases so that the new radius R_g is smaller than the initial radius R_g^0.

$$\frac{S}{k} = \sum_A N_A \left\{ \ln\left[e^{5/2} \frac{V}{N_A} \frac{Z_{\rm int}(A)}{\lambda_T^3(A)} \right] + \frac{\epsilon_A^*(kT)}{kT} \right\} . \tag{2.1}$$

V is the volume of the system and N_A is the number of clusters of A nucleons which are present. $Z_{\rm int}(A)$ is the internal partition function of the cluster and $\epsilon_A^*(T)$ is the energy of internal excitations. The partition function is given by

$$Z_{\rm int}(A) = \sum_{n=0} e^{-\epsilon_n(A)/kT} g_s(n) \tag{2.2}$$

with $\epsilon_n(A)=0$ for the ground state and the sum over the $n=0$ ground state and the $n=1,2,\ldots,$ excited states of the cluster A. $g_s(n)$ is the spin degeneracy factor, which is related to the spin J of a given state n by $g_s(n)=2J+1$. $\lambda_T^3 = h^3/(2\pi M_A kT)^{3/2}$ and comes from the translational motion of the cluster. The mass of the cluster is $M_A \approx m_p A$. The mean excitation energy $\bar{\epsilon}_A^*(T)$ is

$$\bar{\epsilon}_A^*(T) = \frac{\sum_n \epsilon_n e^{-\epsilon_n(T)/kT} g_s(n)}{\sum_n e^{-\epsilon_n(T)/kT} g_s(n)} = \frac{(kT)^2}{Z_{\rm int}} \frac{d}{d(kT)} (Z_{\rm int}(A)) . \tag{2.3}$$

Both $Z_{\rm int}$ and $\bar{\epsilon}^*$ are required in Eq. (2.1) in order to get the correct behavior of the specific heat. The specific heat at constant volume is

$$C_V = \left[\frac{\partial Q}{\partial T} \right]_V = \left[T \frac{\partial S}{\partial T} \right]_V = \sum N_A \left[\frac{3}{2} k + \left[\frac{\partial \epsilon_A^*}{\partial T} \right]_V \right] . \tag{2.4}$$

The first term is the ideal gas specific heat while the second term is the contribution from internal excitations. For example, for an oscillator spectrum the mean excitation energy is

$$\bar{\epsilon}_A^* = \frac{\sum_n nh\nu e^{-nh\nu/kT}}{\sum_n e^{-nh\nu/kT}} = h\nu \frac{x}{1-x} , \tag{2.5}$$

where $x = e^{-h\nu/hT}$. For $kT \gg h\nu$, $\bar{\epsilon}_A^* = kT$ and $C_V = \sum_A \frac{5}{2} N_A k$, as are well known from equipartition arguments.

The value of n runs from 0 to $[A/N_A]$ where $[x]$ is the integer part of x. The choice of the set of N_A's is obtained by maximizing S subject to two constraints. The first constraint fixes the nucleon number to be A_0

$$A_0 = \sum_{A=1}^{A_0} A N_A , \tag{2.6}$$

while the second constraint fixes the total energy to be E

$$E = \sum_{A=1}^{A_0} \left(\tfrac{3}{2} kT + M_A - B_E(A) + \bar{\epsilon}_A^*(T) \right) N_A . \tag{2.7}$$

$B_E(A)$ is the ground-state binding energy of nucleus A. To obtain the maximum entropy we form

$$h = S - \lambda \left[A_0 - \sum A N_A \right] \tag{2.8}$$

and find that choice of N_A's for which the variations $\delta h = 0$ and $\delta E = 0$. The result is

$$\bar{N}_A = \frac{V}{\lambda_T^3} e^{\lambda A - (M_A - B_E(A))/T} Z_{\text{int}}(A) . \tag{2.9}$$

The Lagrange multiplier λ is determined by the constraint equation (2.6).

At this point we pause to mention fluctuations. Because the number of particles in our system is small on a thermodynamic scale, there may be large fluctuations in the value of the thermodynamically determined variables. To get some measure of their importance we look at the multiplicity weight function, ω, which is a measure of the probability that a certain configuration will occur. The entropy S and weight function ω are related by $\omega = e^{S/k}$. Substituting Eq. (2.1) for S we obtain

$$\omega = \prod_A \left[e^{5/2} \frac{V}{N_A} \frac{Z_{\text{int}}}{\lambda_T^3(A)} \right]^{N_A} \exp(\epsilon_A^*(T) N_A / kT) . \tag{2.10}$$

The term $1/\lambda_T^3(A)$ is the translational partition function. Using Stirling's approximation $N! = \sqrt{2\pi N} N^N e^{-N}$, the weight function ω can be written as

$$\omega = \prod_A \left[e^{3/2} V Z_{\text{int}} Z_{\text{trans}} e^{\epsilon_A^*(T)/T} \right]^{N_A} \frac{\sqrt{2\pi N_A}}{N_A!} . \tag{2.11}$$

The above choice of N_A's which maximizes S [given by Eq. (2.9)] also maximizes ω.

The $N_A!$ in Eq. (2.11) is a counting factor associated with the correction for the Gibbs paradox. Volume, temperature, internal excitations, binding energy, and spin effects are also present in this expression. They will be discussed further in the next section.

Neglecting $\sqrt{2\pi N_A}$ compared to $N_A!$ and using the result of Eq. (2.7) for E, Eq. (2.9) for $\bar{N}_A$, and the constraint condition Eq. (2.6), we have rewritten ω in a Poisson-type formula.[19] Specifically, ω is

$$\omega = \left\{ \prod_A \frac{1}{N_A!} (\bar{N}_A)^{N_A} \right\} e^{-\lambda A_0 + E/T} . \tag{2.12}$$

This form for ω makes it easy to study the relative importance of fluctuations away from the most probable partition. Again, using Stirling's approximation we get

$$\omega \simeq \left[\prod_A N_A \left[\frac{\bar{N}_A}{N_A} \right]^{N_A} e^{-N_A} \right] e^{-\lambda A_0 + E/kT}$$

$$= \left[\prod_A N_A \left[\frac{\bar{N}_A}{N_A} \right]^{N_A} \right] \exp\left[-\sum N_A - \lambda A_0 + \frac{E}{kT} \right].$$

Finally, since $\sum N_A = m$ (the multiplicity)

$$\omega = e^{-\lambda A_0 + E/kT} \prod_A N_A \left[\frac{\bar{N}_A}{N_A} \right]^{N_A} e^{-m} .$$

Thus, the ratio of the relative weight of a configuration with N_A nuclei of size A to the maximum weight of all possible configurations is

$$\frac{\omega\{N_A\}}{\bar{\omega}\{\bar{N}_A\}} = \prod_A N_A \left[\frac{\bar{N}_A}{N_A} \right]^{N_A} e^{-\Delta m}$$

$$= \left[\prod_A N_A \left[\frac{\bar{N}_A}{N_A} \right]^{N_A} \right] \exp\left[-\sum (N_A - \bar{N}_A) \right] . \tag{2.13}$$

Here Δm is the change in the multiplicity: $\Delta m = \sum (N_A - \bar{N}_A)$. Thus, we can determine the relative importance of a particular configuration of N_A's knowing only the $\bar{N}_A$'s. One must remember that changes in the cluster numbers are linked by over-all baryon number conservation: $A_0 = \sum A N_A$. A fluctuation in the number of clusters of, for example, size three must be compensated for by a change in the number of clusters of another size (including free nucleons). Number fluctuations of each cluster size are therefore linked.

III. ENERGY OF A NUCLEUS

To explicitly find the $\bar{N}_A$'s we need to know the energy of a nucleus. The free energy $F = U - TS$, so that at $T = 0$ the energy and free energy are equal, and the internal free energy of a nucleus becomes the binding energy of a nucleus with A nucleons. For the $T = 0$ binding energy we will take the Myers-Swiatecki expression for a spherical nucleus[20]

$$B_E(A) = a_v A - a_s A^{2/3} - a_k A^{1/3} - a_c Z^2 A^{-1/3} - \frac{(N-Z)^2}{A^2} a_{sy} A - \frac{(N-Z)^2}{A^2} a_{sy}^s A^{2/3} \cdots , \tag{3.1}$$

where the volume term $a_v = 15.96$ MeV, the surface term $a_s = 20.69$ MeV, the Coulomb term $a_c = \frac{3}{5} e^2 / r_0 = 0.73$ MeV, the volume symmetry term $a_{sy} = 36.8$ MeV and the surface symmetry term $a_{sy}^s = 17.8$ MeV. At $T = 0$ the curvature correction term a_k is very small and hard to extract from known binding energies, therefore *at* $T = 0$ it is set equal to zero. In this paper we will neglect the effects of the symmetry terms and consider only volume, surface, and Coulomb effects and the curvature correction term.

For a heated liquid drop the energy is replaced by the free energy and the coefficients of the liquid drop expression become temperature dependent. Specifically we write

$$F(T)=F_V(T)+F_S(T)+F_C(T)+F_k(T)\ ,$$

where F_V is the volume free energy, F_S is the surface free energy, F_C is the Coulomb free energy, and F_k is the curvature correction term to the free energy. We now consider each of these terms separately.

A. Volume term

The volume term represents all energies which go linearly with A. In a Fermi gas model it includes the internal energy of the nucleus as well as the binding of the nucleons. To calculate the internal energy we start with the level density of excited states of energy ϵ in a nucleus of size A (Ref. 21).

$$\rho(\epsilon)=\frac{c}{a^{1/4}\epsilon^{5/4}}e^{2\sqrt{a\epsilon}}\ . \tag{3.2}$$

Here $c=\sqrt{\pi}/12$. $a=A/\epsilon_0$ is related to the density of states at the Fermi energy by $a=(\pi^2/6)(dn/d\epsilon)_{\epsilon=\epsilon_F}$. For a Fermi gas $(dn/d\epsilon)_{\epsilon=\epsilon_F}=3A/2\epsilon_F$ so $a=(\pi^2/4\epsilon_F)A$ and $\epsilon_0=4\epsilon_F/\pi^2$. In a harmonic oscillator description $dn/d\epsilon$ equals the degeneracy of the last shell divided by the spacing $h\nu$ and $a\approx A/10$ MeV. Surface corrections to a have been discussed by Fai and Randrup, these change a to[2]

$$a=\frac{A}{8\ \text{MeV}}\left[1-\frac{k_2}{A^{1/3}}\right]$$

with $k_2=0.8$.

In a Fermi gas model the quantity ϵ_0 is about twice the experimental result, with $\epsilon_0=16$ MeV in the model and $\epsilon_0=8$ MeV from experimental level densities. ϵ_0 is also related to the kinetic energy per nucleon through $\epsilon_F=\frac{3}{5}E_K$.[22] For a Fermi gas with $E_K=20$ MeV, $\epsilon_0=(20/3\pi^2)E_K=13.52$ MeV.

From a saddle point integration we find the internal partition function[23]

$$Z_{\text{int}}=\int\rho(\epsilon)e^{-\beta\epsilon}d\epsilon\approx c\sqrt{\pi}\frac{e^{akT}}{akT}\ . \tag{3.3}$$

The mean excitation energy is then

$$\bar{\epsilon}^*=-\frac{1}{Z_{\text{int}}}\frac{\partial Z_{\text{int}}}{\partial\beta}\approx\frac{A}{\epsilon_0}(kT)^2=\frac{\pi^2}{4\epsilon_F}A(kT)^2\ , \tag{3.4}$$

where $\beta=1/kT$. The bulk free energy then goes to

$$F_V=-a_v A-a(kT)^2=-\left[a_v+\frac{(kT)^2}{\epsilon_0}\right]A\ . \tag{3.5}$$

This is the expression for the bulk free energy used by Bondorf, *et al.*[4]

The level density as given by Eq. (3.2) has no cutoff, with the result that the partition function increases exponentially with temperature as e^{akT}/akT. While this may model the behavior of nuclei at low temperatures, the behavior at high temperature requires the introduction of some cutoff procedure. Most cutoff procedures are somewhat arbitrary. One prescription, which we adopt, includes an exponential decrease $e^{-\beta_0\epsilon}$ where $\beta_0=1/kT_0$ is a limiting temperature.[3] The partition function then becomes

$$Z_{\text{int}}=\int\rho(\epsilon)e^{-\beta\epsilon}e^{-\beta_0\epsilon}d\epsilon\approx c\sqrt{\pi}\frac{e^{akTT_0/(T+T_0)}}{akTT_0/(T+T_0)}\ , \tag{3.6}$$

and the mean excitation $\bar{\epsilon}^*_A$ is then

$$\bar{\epsilon}^*_A\approx a(kT)^2\left[\frac{T_0}{T+T_0}\right]^2\ . \tag{3.7}$$

The bulk free energy is given by the expression

$$F_V=-a_v A-\frac{A}{\epsilon_0}(kT)^2\left[\frac{T_0}{T+T_0}\right]=-a_v(T)A\ , \tag{3.8}$$

with

$$a_v(T)=a_v+\frac{(kT)^2}{\epsilon_0}\left[\frac{T_0}{T+T_0}\right]\ . \tag{3.9}$$

The temperature dependences of Z_{int} and $\bar{\epsilon}^*$ are now bounded, reaching limiting values

$$\lim_{T\to\infty}Z_{\text{int}}=c\sqrt{\pi}\frac{e^{akT_0}}{akT_0}\ \text{and}\ \lim_{T\to\infty}\bar{\epsilon}^*=a(kT_0)^2\ .$$

B. Surface term

When a nucleus is heated, nucleons evaporate from it and form a vapor; the boundary separating the nucleus from this vapor has an associated surface energy. As the temperature is increased, the density of nucleons in the vapor increases while the density of the liquid decreases. Eventually a temperature is reached where the liquid and vapor densities are equal and a surface no longer exists between the liquid and vapor. At this critical temperature T_c the surface energy must go to zero. Furthermore, in a mean-field theory it should go to zero as $|T_c-T|^{3/2}$.

Here we take the surface free energy to vary with temperature as

$$F_S=4\pi R^2\sigma(T)\ ,$$

with the radius of the nucleus $R=r_0A^{1/3}$ and the surface tension coefficient $\sigma(T)$ given by[24]

$$4\pi r_0^2\sigma(T)=a_s\left[1+\frac{3}{2}\frac{T}{T_c}\right]\left[1-\frac{T}{T_c}\right]^{3/2} \tag{3.10}$$

For low T the surface free energy varies quadratically with T, as predicted by Thomas-Fermi theory. For T near T_c it goes to zero as $|T_c-T|^{3/2}$. At $T=0$, F_S equals the surface energy term in the liquid drop binding energy, thus a_s in Eq. (3.10) is the same as a_s in the Myers-Swiatecki mass formula, Eq. (3.1): $a_s=20.69$ MeV.

C. Curvature energy term

In the Myers-Swiatecki generalization of the Weissäcker mass formula, the term proportional to $A^{1/3}$ is a curvature correction term. We note here that $A^{1/3} \approx \ln A$ for $A \approx 10$ to 300, so that one could have used a ln A behavior as well. At low temperatures these higher order terms, either $A^{1/3}$ or $\ln A$, are hard to extract from known binding energies since the larger volume and surface terms dominate the mass formulas. Near a critical point, however, the higher order terms become important.

In the Fisher droplet model the curvature energy near a critical point is taken to be

$$F_k = \tau k T \ln A \tag{3.11}$$

and results in a curvature correction to the entropy S. (Recall $F = U - TS$.) τ is not a free parameter, but is determined by critical exponent theory. In a mean-free theory $\tau = 2\frac{1}{3}$.

D. Coulomb term

For an isolated sphere with uniform charge Ze, the Coulomb energy is simply

$$E_C = \frac{3}{5}\frac{Z^2 e^2}{R} ,$$

with $R = r_0 A^{1/3}$. When a charged nuclear liquid drop is heated, a vapor forms and surrounds the drop. Since the vapor contains protons, the Coulomb energy is modified by the interaction of the localized liquid drop with the vapor. The total Coulomb energy involves the interaction energy of charges inside the drop with each other, $E_C(d \otimes d)$, charges inside the drop with charges in the vapor, $E_C(d \otimes v)$, and charges in the vapor with each other, $E_C(v \otimes v)$. Let $\xi_l(Z)$ be the charge density of the liquid drop, $\xi_g(Z)$ the charge density of the gaseous vapor, R_l the radius of the liquid drop, and R_g the radius of the vapor, as shown in Fig. 1(b). The Coulomb energy of the drop charges interacting with each other is still

$$E_C(d \otimes d) = \frac{3}{5}\frac{Z^2 e^2}{R_l} = \frac{3}{5}\xi_l^2(Z)\left[\frac{4\pi}{3}\right]^2 R_l^5 . \tag{3.12}$$

The Coulomb energy of the charges in the drop interacting with those in the vapor is

$$E_C(v \otimes v) = \frac{3}{5}\xi_l^2(\mathbf{Z})\xi_g(\mathbf{Z})\left[\frac{4\pi}{3}\right]^2 \times R_l^3(R_g - R_l)(2R_g + 3R_l) , \tag{3.13}$$

and the Coulomb energy of the vapor charges interacting with each other is

$$E_C(v \otimes v) = \frac{3}{5}\xi_g^2(Z)\left[\frac{4\pi}{3}\right]^2 (R_g - R_l)^2 \times (R_g + R_l)(R_g^2 + R_g R_l + 2R_l^2) . \tag{3.14}$$

The total Coulomb energy is $E_C = E_C(d \otimes d) + E_C(d \otimes v) + E_C(v \otimes v)$. In Eqs. (3.13) and (3.14) we let the nucleus form at an arbitrary point inside the vapor and then average over the volume of the vapor.

Figure 1 also illustrates the Coulomb energy fluctuation when a drop is formed from and in a uniform vapor. Let R_g^0 be the radius of the vapor without the charged drop and $Z_0 e$ be the total charge of the vapor, as shown in Fig. 1(a). Then the Coulomb energy of the vapor alone is

$$E_C(v_0 \otimes v_0) = \frac{3}{5}\frac{Z_0^2 e^2}{R_g^0} = \frac{3}{5}\xi_g^2(Z)\left[\frac{4\pi}{3}\right]^2 (R_g^0)^5 . \tag{3.15}$$

The vapor density is understood to be the same with and without the drop. Since the drop is more dense than the vapor $R_g^0 > R_g$. The fluctuation in the Coulomb energy caused by the formation of the drop is then $\delta E_C = E_C(d \otimes d) + E_C(d \otimes v) + E_C(v \otimes v) - E_C(v_0 \otimes v_0)$, which can be rewritten as

$$\delta E_C = \frac{3}{5}(\chi e)^2\left[\frac{4\pi}{3}\right]^2 \{R_l^3(\rho_l - \rho_g)[R_l^2\rho_l + \rho_g(R_g^2 + R_g R_l - 2R_l^2)] - \rho_g^2[(R_g^0)^5 - R_g^5]\} , \tag{3.16}$$

ρ_l and ρ_g are the matter densities in each phase, and $\chi = Z/A$ so that $\xi_l = \chi e \rho_l$ and $\xi_g = \chi e \rho_g$. In this paper we will take $\chi = \frac{1}{2}$ for simplicity. Note that in the limit $\rho_l = \rho_g$, then $R_g^0 = R_g$ and $\delta E_C \to 0$, thus the Coulomb fluctuation goes to zero at the critical point.[25]

The temperature dependence of the Coulomb energy can be established by considering ρ_l and ρ_g to be the densities in a liquid-gas phase transition. For such a situation ρ_l and ρ_g are determined as the endpoints of a Maxwell construction in a pressure versus volume per particle $(1/\rho)$ plot of the nuclear equation of state. In Sec. IV A we present a simple analytic model of such a phase transition. For now we give the results for ρ_l and ρ_g

$$\tilde{\rho}_l = \frac{\rho_l}{\rho_c} = \tfrac{3}{2} - \tfrac{1}{2}\tilde{T} + \tfrac{3}{2}\sqrt{(1-\tilde{T})(1+\tilde{T}/3)}$$

and (3.17)

$$\tilde{\rho}_g = \frac{\rho_g}{\rho_c} = \tfrac{3}{2} - \tfrac{1}{2}\tilde{T} - \tfrac{3}{2}\sqrt{(1-\tilde{T})(1+\tilde{T}/3)} ,$$

where the reduced temperature $\tilde{T} = T/T_c$ and ρ_c is the critical density of the system. These results are discussed further in Sec. IV A. Note that they depend only on the ratio of T/T_c.

Using the above equations we calculate the Coulomb energy of a drop imbedded in a vapor as follows. Given the reduced temperature $\tilde{T}$ and critical density ρ_c, the

drop and vapor densities ρ_l and ρ_g are determined by the coexistence curve endpoints. R_l is determined by

$$\tfrac{4}{3}\pi R_l^3=\frac{2Z_l}{\rho_c\tilde{\rho}_l} . \tag{3.18}$$

Once R_l is determined, we can find R_g from

$$\tfrac{4}{3}\pi(R_g^3-R_l^3)=\frac{2(Z_0-Z_l)}{\rho_c\tilde{\rho}_g} . \tag{3.19}$$

To get R_g^0 we solve

$$\tfrac{4}{3}\pi(R_g^0)^3=\frac{2Z_0}{\rho_c\tilde{\rho}_g} . \tag{3.20}$$

In these equations we have let $\chi=Z/A=\frac{1}{2}$. Then the Coulomb energy E_C and fluctuation δE_C when a drop of charge Z_l forms in a vapor of charge Z_0-Z_l follow from Eqs. (3.12) through (3.16).

IV. NUCLEAR LIQUID-GAS PHASE TRANSITIONS

A macroscopic description of the appearance of a liquid-gas phase transition appropriate for heavy-ion collisions has been discussed by Bertsch and Siemens.[26] In their approach, a nuclear collision first produces compressed and heated nuclear matter. The matter then expands isentropically until the system enters the unstable region of the pressure-density phase diagram. At this point instabilities can grow and split the system into a liquid and gas phase, the endpoints of the Maxwell construction line in the phase diagram. Again, a state of lowest free energy is produced. In our scenario the system never enters the unstable region. Instead it expands into the metastable region, at which point we get a liquid-gas phase transition.

A. A simple model and its ferromagnetic correspondence

We start with a very simple expression for our equation of state, which is both easy to work with and useful in illustrating the gross behavior of the system. The equation of state that we use contains three terms. One term represents the pressure from the kinetic motion of the nucleons and is taken to be ρkT, where ρ is the density. The other two terms come from the interaction energy, with one term attractive and the other term repulsive. (The repulsive term manifests itself at higher densities and represents the short range repulsion between nucleons.) Specifically, we have

$$P=\rho kT-a_0\rho^2+2a_3\rho^3 , \tag{4.1}$$

a_0 and a_3 are parameters of the theory. If we assume a Skyrme interaction among the nucleons we can write $a_0=(2E_B+\frac{4}{3}E_K)/\rho_0$ and $a_3=(E_B+\frac{1}{3}E_K)/\rho_0^2$. (This equation of state and the parameters a_0 and a_3 are discussed more fully in Ref. 22.) The critical point occurs at ρ and T for which $\partial P/\partial\rho=0$ and $\partial^2P/\partial^2\rho=0$. The critical temperature is $kT_c=a_0^2/6a_3$ and the critical density is $\rho_c=a_0/6a_3$. If we take $E_B=8$ MeV for the binding energy per nucleon, $E_K=20$ MeV for the average kinetic energy of a nucleon, and $\rho_0=0.16$ fm^{-3} for the ground-state density of a nucleus, then $a_0=266.7$ MeV-fm^3 and $a_3=572.92$ MeV-fm^6, so $kT_c=20.69$ MeV and $\rho_c=0.078$ fm^{-3}.

The endpoints of the Maxwell construction line are easily determined. In a P-V diagram, it is drawn so that the shaded areas are equal, as illustrated in Fig. 2. The Gibbs condition of phase equilibrium, equality of the chemical potentials and pressures between the phases, is automatically satisfied by this construction. The pressure equality gives

$$\rho_g kT-a_0\rho_g^2+2a_3\rho_g^3=\rho_l kT-a_0\rho_l^2+2a_3\rho_l^3 , \tag{4.2}$$

while the chemical potential equality results in

$$kT\ln\rho_g-2a_0\rho_g+3a_3\rho_g^2=kT\ln\rho_l-2a_0\rho_l+3a_3\rho_l^2 , \tag{4.3}$$

l stands for the liquid phase, g for the gas phase. In the last result we have used the Gibbs-Duheim equation $d\mu=(1/\rho)dP$ for $dT=0$. Defining reduced quantities $\tilde{\rho}=\rho/\rho_c$, $\tilde{T}=T/T_c$, and

$$2\sigma=\tilde{\rho}_l+\tilde{\rho}_g, \quad 2\eta=\tilde{\rho}_l-\tilde{\rho}_g \tag{4.4}$$

allows us to rewrite the pressure and chemical potential equations as

$$\eta^2=3[\sigma(2-\sigma)-\tilde{T}] , \tag{4.5}$$

and

$$\frac{\eta}{\sigma}=\tanh\left[\frac{\eta(2-\sigma)}{\tilde{T}}\right] . \tag{4.6}$$

Here we have used the equality $(\frac{1}{2})\ln[(1+x)/(1-x)]=\tanh^{-1}x$.

The coupled equations for η and σ can be solved numerically and the results used to find $\tilde{\rho}_l$ and $\tilde{\rho}_g$. The numerical solutions are plotted as solid lines in Fig. 3. The dashed lines are plots of the equations

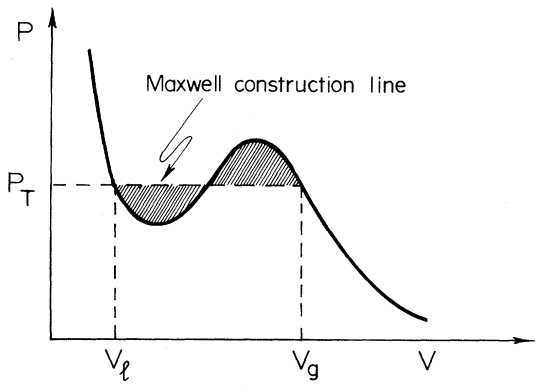

FIG. 2. P-V diagram for a liquid-gas phase transition. The Maxwell construction line is parallel to the volume axis and is drawn such that the areas of the shaded regions are equal. It gives the pressure P_T at which the phase transition occurs. The intercepts of the Maxwell line with the pressure volume curve give the volumes of the liquid (V_l) and gas (V_g).

$$\sigma=\tfrac{3}{2}-\tfrac{1}{2}\tilde{T},\quad \eta=\sqrt{\tfrac{3}{4}(1-\tilde{T})(3+\tilde{T})}\ . \tag{4.7}$$

As can be seen, these approximate solutions are exceedingly accurate. [In fact, they exactly satisfy Eq. (4.5), but only approximately satisfy Eq. (4.6). The solutions have the added feature that the behavior of σ and η near $\tilde{T}=1$, the critical point, is that which is predicted by critical exponent theory in a mean-field approximation.] If we use Eqs. (4.7), then $\tilde{\rho}_l$ and $\tilde{\rho}_g$ are given by

$$\tilde{\rho}_l=\frac{\rho_l}{\rho_c}=\tfrac{3}{2}-\tfrac{1}{2}\tilde{T}+\tfrac{3}{2}\sqrt{(1-\tilde{T})(1+\tilde{T}/3)}$$

and (4.8)

$$\tilde{\rho}_l=\frac{\rho_g}{\rho_c}=\tfrac{3}{2}-\tfrac{1}{2}\tilde{T}-\tfrac{3}{2}\sqrt{(1-\tilde{T})(1+\tilde{T}/3)}\ .$$

These are the equations introduced in Sec. III D.

Equation (4.6), for the behavior of the cord length η, is in many ways similar to that for the magnetization M in a ferromagnet. By letting N be the number of atoms which can have magnetic moment $\pm\mu$ in the presence of an external field B, the net magnetization M is[27]

$$M=N\mu\tanh\frac{\mu B}{T}\ .$$

In a mean-field theory of ferromagnetism $B=\lambda M$ and the equation that governs the spontaneous magnetization is[27]

$$\frac{M}{N\mu}=\tanh\frac{\mu\lambda M}{T}\ .$$

Defining a reduced magnetization $m=M/N\mu$ and a reduced temperature $t=T/\mu^2\lambda N=T/T_c$, the previous equation becomes

$$m=\tanh\frac{m}{t}\ . \tag{4.9}$$

Comparing Eqs. (4.6) and (4.9) shows that for $\sigma=1$ ($T=\tilde{T}$), η and m obey the same equation. Thus, there exists a strong correspondence between η, the cord length between the Maxwell endpoints, and m, the spontaneous magnetization. The behavior of σ is actually $\sigma=3/2-\tilde{T}/2$ over a large range of $\tilde{T}$, so the liquid-gas transition equations are somewhat more complicated.

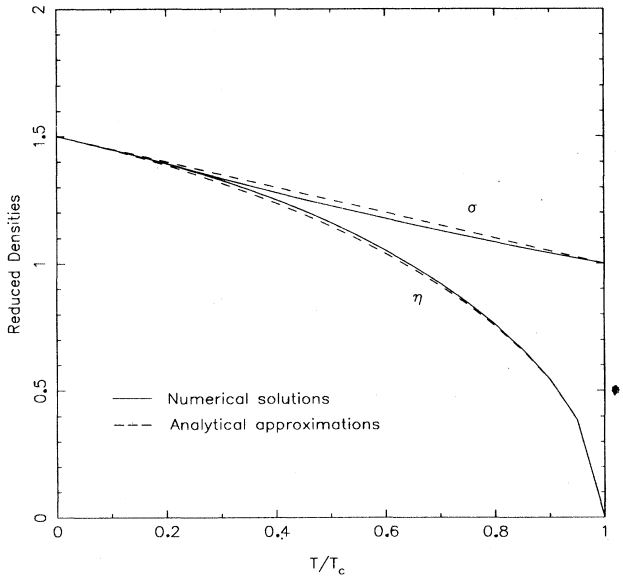

FIG. 3. Reduced densities η and σ vs T/T_c in an uncharged vapor with no surface energy. The solid lines show the numerical solutions of the transcendental equations for η and σ, the dashed lines plot the approximations to η and σ given in the text.

B. Surface and Coulomb effects

Surface effects can be included in the above prescription by considering the change in the Gibbs conditions due to the finite size of nuclei. Specifically, the differences in liquid and vapor pressures across the boundary are related to the surface tension by

$$\delta P=\frac{\partial F_S}{\partial V}=\frac{2\sigma(T)}{R}\ , \tag{4.10}$$

where R is the radius of the drop and $\sigma(T)$ is the temperature dependent surface tension. No change in chemical potential across the surface occurs in this case. When we include Eq. (4.10) in the right-hand side of Eq. (4.2) then the equations for η and σ become

$$\frac{\eta}{\sigma}=\tanh\left[\frac{\eta(2-\sigma)}{\tilde{T}}\right] \tag{4.11}$$

and

$$\eta\left[\tilde{T}-2\sigma+\sigma^2+\frac{\eta^2}{3}\right]=\frac{\tilde{\sigma}(T)}{A^{1/3}}(\sigma+\eta)^{1/3}\ . \tag{4.12}$$

Here A is the mass number of the drop and $\tilde{\sigma}(T)$ is a dimensionless surface tension given by $\tilde{\sigma}(T)=\sigma(T)(4\pi/3)^{1/3}/(T_c\rho_c^{2/3})$. Near the critical point $\tilde{\sigma}(T)\to 0$ and one recovers the earlier results as required. The finite size effects change the shape of the coexistence curve, as was first noted by Bonche and Levit.[28] Our analysis gives an explicit expression for this change. Finite size effects on the critical point were discussed in Ref. 22.

One can also consider Coulomb effects on the coexistence conditions[28,29] and on the critical point.[22] If we ignore interactions with the vapor and take the Coulomb energy of a nuclear drop to be that of an isolated sphere, then $E_C=3/5Z^2e^2/R$. The analysis in this case is simple, but the final equations for η and σ are somewhat complicated. The Coulomb interaction produces a contribution to both the chemical potential and pressure differences across the surface. The equation coming from the chemical potential and involving the hyperbolic tangent now reads

$$A\left[\eta\sigma-2\eta+\tilde{T}\tanh^{-1}\frac{\eta}{\sigma}\right]=\frac{2}{T_c}\left[\frac{4\pi}{3}\right]^{1/3}\frac{6e^2\rho_c^{1/3}}{5}\frac{Z^2}{A^{4/3}}(\sigma+\eta)^{1/3}\ . \tag{4.13}$$

The pressure equation now becomes

$$\eta\left[\tilde{T}-2\sigma+\sigma^2+\frac{\eta^2}{3}\right]=\frac{\tilde{\sigma}(T)}{A^{1/3}}(\sigma+\eta)-\frac{1}{2}\left[\frac{4\pi}{3}\right]^{1/3}\left[\frac{e^2}{5r_0T_c}\right]\rho_c^{1/3}\frac{Z^2}{A^{4/3}}(\sigma+\eta)^{4/3}\ , \tag{4.14}$$

where the first term on the right-hand side of the previous equation comes from the surface tension, while the second term is the Coulomb contribution.

In the analysis of Bonche and Levit, based on this simple form for the Coulomb interaction, the system develops a Coulomb instability before the critical point is reached. Their solution shows a system of bound neutrons left behind with a vapor of protons pressed against the walls of a box in which the calculations are performed. Here we point out that symmetry forces, which want to restore the equality of protons and neutrons, will resist this type of solution. Moreover, symmetry forces make a system of neutrons unbound, as can easily be seen from the Weiszäcker mass formula. An analysis of the effect of Coulomb forces including drop-vapor interactions on the coexistence curve will be given in a future study. Now, however, we shall study their effect on nuclear clustering and fragmentation yields.

V. GROWTH OF LARGE CLUSTERS IN A MAXIMUM ENTROPY APPROACH

A. Conditions for growth

A model for finding the composition of a nuclear system is terms of nucleons and clusters in an approach which maximize the entropy was established in Sec. II. A condition for the system to favor the formation of large clusters is $\bar{N}_{A+1}/\bar{N}_A \geq 1$, where $\bar{N}_A$ and $\bar{N}_{A+1}$ are the number of clusters of sizes A and $A+1$ which maximizes the entropy as given by Eq. (2.9). If this condition is satisfied then a cluster of mass number $A+1$ will be more abundant than one of mass number A. If $\bar{N}_A$ were given by a power series in A, so that $\bar{N}_A \sim x^A$, then $x>1$ would be the condition necessary to favor the formation of large clusters. In this section we shall use this condition to analyze the system in the case where the Coulomb energy is treated as an isolated, uniformly charged drop, and the presence of the vapor is ignored [i.e., $E_C(d\otimes v)=E_C(v\otimes v)=0$].

We start by writing

$$\bar{N}_A=CA^{3/2}(e^{\lambda' A-(\beta_s(T)A^{2/3}-\beta_C(T)A^{5/3})/kT})e^{-F_{\rm int}(A)/kT}\ , \tag{5.1}$$

where we have used the connection between the internal free energy $F^{\rm int}$ and the internal partition function, $Z_{\rm int}=e^{-F_{\rm int}/kT}$. $\lambda'=\lambda-(m_p-a_v)/kT$ and $\beta_s=4\pi r_0^2\sigma(T)=a_s(1+3T/2T_c)(1-T/T_c)^{3/2}$ with $\sigma(T)$ the temperature dependent surface tension coefficient. $\beta_C(T)A^{5/3}$ is the Coulomb energy with $\beta_C=(\frac{3}{5}\chi^2e^2/r_0)$. The internal partition function is given by Eq. (3.3), $Z_{\rm int}=(c\sqrt{\pi})e^{akT}/akT$. Thus, we can write $\bar{N}_A$ as

$$\bar{N}_A=D_T\frac{x^A y^{A^{2/3}} z^{A^{5/3}}}{A^{\tau_{\rm eff}}}\ , \tag{5.2}$$

where

$$\begin{aligned} x&=\exp\left[\lambda-\frac{m_p-a_v}{kT}+\frac{kT}{\epsilon_0}\right]\ ,\\ y&=e^{-\beta_s(T)/kT}\ ,\\ z&=e^{-\beta_C/kT}\ , \end{aligned} \tag{5.3}$$

and

$$\tau_{\rm eff}=\tau-\tfrac{1}{2}\ .$$

The "$-\frac{1}{2}$" in $\tau_{\rm eff}$ comes from the thermal motion of the clusters, which produces the $1/\lambda_T^3$ factor in $\bar{N}_A$ of Eq. (2.9) and the $1/a$ behavior of the internal partition function. Thus, the translational and internal excitation effects act to reduce the critical exponent by 0.5. When the evaluation of the internal partition function includes an exponential cutoff, kT/ϵ_0 is replaced by $kT(T_0/T+T_0)/\epsilon_0$, so that

$$x=\exp\left[\lambda-\frac{m_p-a_v}{kT}+\frac{kT}{\epsilon_0}\left[\frac{T_0}{T+T_0}\right]\right]\ . \tag{5.4}$$

Since y and z are always less than unity, $x<1$ implies that $\bar{N}_{A+1}/\bar{N}_A$ will always be decreasing. Therefore, a necessary (but not sufficient) condition for the system to favor the presence of large cluster is $x>1$, or

$$\lambda-\frac{m_p-a_v}{kT}+\frac{kT}{\epsilon_0}f(T)>0\ . \tag{5.5}$$

Here $f(T)=1$ with no cutoff and $f(T)=T_0/(T+T_0)$ with an exponential cutoff in the evaluation of $Z_{\rm int}$. A sample calculation of the relative yield of clusters as a function of A is presented in Fig. 4 and discussed further in the next section.

The critical size cluster is that for which $\bar{N}_A$ is a minimum. So long as this is much less than the total size of the system there will be a good probability for the formation of large clusters. Neglecting for a moment the Coulomb term, the critical size droplet has a mass num-

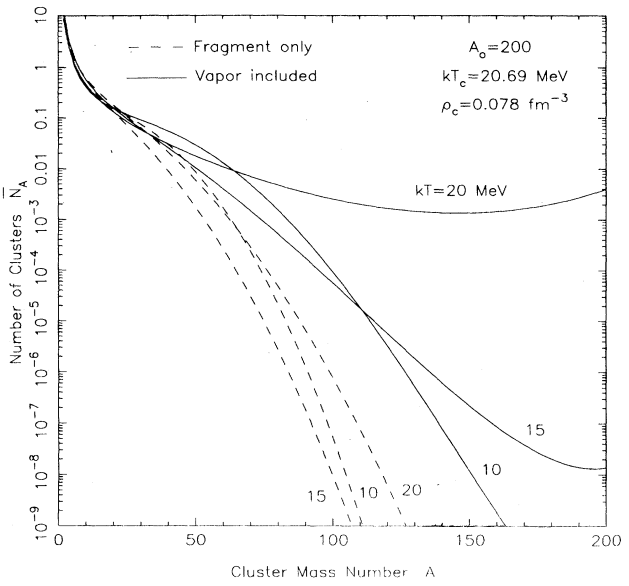

FIG. 4. Cluster production from a system of 200 nucleons as a function of the cluster nucleon number. The results are plotted for the case in which only the charge of the cluster is considered (dashed curves) and the case in which the complete Coulomb energy is used (solid curves). Results are plotted for $kT=10$, 15, and 20 MeV. (At $kT=20$ MeV $\rho_g/\rho_l \approx \frac{1}{2}$.)

ber A_c given by

$$\frac{xy^{(A_c+1)^{2/3}}}{y^{(A_c)^{2/3}}}=1 , \tag{5.6}$$

which, for $A_c \gg 1$, can be reduced to

$$A_c^{1/3}=-\frac{\frac{2}{3}\ln y}{\ln x} . \tag{5.7}$$

When the expressions for x and y are substituted into the right-hand side of the last equation, we recover the results of classical nucleation theory,[30]

$$A_c^{1/3}=\frac{2\sigma(T)}{r_0(\mu_g-\mu_l)\rho_l}$$

where $r_0=(3/4\pi\rho_l)^{1/3}$.

B. Numerical studies

In this section we repeat the analysis of Sec. V A, now including the effects of the vapor on the Coulomb energy. In this case E_C is no longer a simple sum of powers of A, so we can no longer write $\bar{N}_A$ as a power series in A. Thus, we replace the analytical expressions of the previous section with numerical solutions for $\bar{N}_A$. Briefly, we use our expressions for the complete Coulomb energy with Eq. (2.9) for $\bar{N}_A$ to find $\bar{N}_A$ in terms of λ and T. Using this result in the constraint equation $A_0=\sum_A A\bar{N}_A$ gives us λ, we then have $\bar{N}_A$ as a function of T. A more detailed explanation of this procedure can be found in Ref. 8. We have improved the calculations done in that paper by including the surface curvature term in the energy and a cutoff in the internal partition function at the critical temperature. We have also allowed the densities of both the vapor and cluster to vary with temperature according to Eqs. (4.8).

Figure 4 shows the results of our calculations for a system of 200 nucleons at various temperatures. The figure plots the number of clusters of size A which are formed in one collision as a function of A. The solid lines are our results using the complete Coulomb energy. For comparison we also plot, as the dashed curves, the same calculations using the isolated drop Coulomb energy.

At temperatures up to $T\approx 3T_c/4$ both forms of the Coulomb energy result in yields which are strongly peaked at low mass number; the effects of the vapor are relatively weak. Even above this temperature the yields calculated using the Coulomb energy of an isolated drop continue to fall exponentially with A, this corresponds to $x<1$ in the previous section. However, when the complete Coulomb energy is used the yields show a systematic change with temperature. As T increases so do the large A yields, and the fragmentation curves become U shaped. Vapor effects become prominent and begin to favor the formation of large nuclei at high temperature.

To understand why the yields behave in this way we need to reexamine Eqs. (4.8) for the liquid and vapor densities. At $T=0$, and $\rho_g=0$ we expect the vapor to have little effect. In fact, $\rho_g \ll \rho_l$ for most $\tilde{T}$; $\rho_g/\rho_l=0.1$ at $\tilde{T}=0.70$ and $\rho_g/\rho_l=\frac{1}{2}$ at $\tilde{T}=0.96$. Thus, it is not until T gets close to T_c that the effects of the vapor are noticeable. When we charge the vapor the contributions from $E_C(d\otimes v)$ and $E_C(v\otimes v)$ increase the total energy and hence decrease the yields. Since there is more vapor around small clusters, will be greater at lower mass number. Conservation of baryon number does not allow the yield to fall across all baryon number. Thus, the decrease in the number of small clusters is compensated for by an increase in the number of large clusters, and the fragmentation yields become U shaped as T approaches T_c.

VI. CONCLUSIONS

We have presented a method for calculating fragment yields in heavy-ion collisions which starts with a thermalized gas of unbound nucleons. Fluctuations in the gas will cause these nucleons to cluster, if the binding forces are large enough the clusters will remain bound and become nuclei. How often nuclei of a particular size form is determined by the requirement that the entropy be maximized, subject to conservation of energy and baryon number. To calculate this energy we used the Myers-Swiatecki equation for the energy of a spherical nucleus generalized to nonzero temperatures. We also used a form for the Coulomb energy which accounts for the presence of the vapor. Finally, the densities and temperature of the system were related through a virial expansion equation of state. The results for the liquid and gas densities in an uncharged system with no surface resemble the behavior of the magnetization of a ferromagnet in a magnetic field.

As an example of our method we calculated the relative yield of nuclei from a system of 200 nucleons at tem-

perature of 10, 15, and 20 MeV. We did the calculations both with and without Coulombic contributions from the thermalized gas so that we might study the importance of such contributions. We found that ignoring the vapor resulted in yields which fell exponentially with A over the entire range of temperature $0 \leq T \leq T_c$. However, including the vapor caused the yields to exhibit a marked dependence on temperature. In this case the yields progressed from an exponential decrease to a powerlaw decrease to a relatively flat curve with a shallow minimum as the temperature increased and approached T_c. This high temperature behavior resembles the experimental results from A-A collisions, thus the picture of a liquid nucleus forming within a vapor of nucleons may be a valid one with which to calculate heavy-ion fragmentation yields.

ACKNOWLEGMENTS

We would like to acknowledge the help of Joe Sak in clarifying many of these ideas. This work was supported by the National Science Foundation through Grant No. PHY 87-01597 and by a Rutgers University Supercomputer Fellowship.

[1]J. Randrup and S. Koonin, Nucl. Phys. **A356**, 223 (1981).
[2]G. Fai and J. Randrup, Nucl. Phys. **A381**, 557 (1982); **A404**, 551 (1983).
[3]S. Koonin and J. Randrup, Nucl. Phys. **A474**, 173 (1987).
[4]J. Bondorf, R. Donangelo, I. Mishustin, C. Pethick, H. Schulz, and K. Sneppen, Nucl. Phys. **A443**, 321 (1985); J. Bondorf, R. Donangelo, I. Mishustin, H. Schulz, Nucl. Phys. **A444**, (1985) 460.
[5]J. Aichelin and J. Hufner, Phys. Lett. **136B**, 15 (1984); J. Aichelin, J. Hufner, and R. Ibarra, Phys. Rev. C **30**, 107 (1984).
[6]D. H. E. Gross, L. Sapathy, M. Ta-chung, and M. Sapathy, Z. Phys. A **309**, 41 (1982); D. H. E. Gross, Phys. Scr. **T5**, 213 (1983); D. H. E. Gross and X. Zhang, Phys. Lett. **161B**, 47 (1985).
[7]G. Fai and A. Mekjian, Phys. Lett. **169B**, 281 (1987).
[8]A. R. DeAngelis, A. Z. Mekjian, and G. Fai, RU-88-21 (submitted to Phys. Lett. B).
[9]G. Baym, H. Bethe, and C. Pethick, Nucl. Phys. **A175**, 225 (1971).
[10]H. Bethe, G. E. Brown, J. Applegate, and J. M. Lattimer, Nucl. Phys. **A324**, 487 (1979).
[11]W. A. Friedman and W. G. Lynch, Phys. Rev. C **28**, 950 (1983).
[12]A. Z. Mekjian, Phys. Rev. C **17**, 1051 (1978).
[13]J. Gossett, J. I. Kapusta, and G. D. Westfall, Phys. Rev. C **18**, 844 (1978).
[14]R. Bond, P. J. Johansen, S. E. Koonin, and S. Garpman, Phys. Lett. **71B**, 43 (1977).
[15]S. DasGupta and A. Z. Mekjian, Phys. Rep. **C72**, 132 (1981).
[16]J. E. Finn, S. Agarwal, A. Bujak, J. Chuang, L. J. Gutay, A. S. Hirsch, R. W. Minich, N. T. Porile, R. P. Scharenberg, B. C. Stringfellow, and F. Turkot, Phys. Rev. Lett. **49**, 1321 (1982); R. W. Minich, S. Agarwal, A. Bujack, J. Chuang, J. E. Finn, L. J. Gutay, A. S. Hirsch, N. T. Porile, R. P. Scharenberg, B. C. Stringfellow, and F. Turkot, Phys. Lett. **118B**, 458 (1982).
[17]M. E. Fisher, Physics (N.Y.) **3**, 255 (1967).
[18]P. Morse, *Thermal Physics* (Benjamin, Reading, Massachusetts, 1969).
[19]G. Cecil, S. DasGupta, and A. Z. Mekjian, Phys. Rev. C **20**, 1021 (1979).
[20]W. Myers and V. Swiatecki, Nucl. Phys. **81**, 1 (1966); Ann. Phys. (N. Y.) **55**, 395 (1969).
[21]A. Bohr and B. Mottleson, *Nuclear Structure* (Benjamin, New York, 1969), Vol. I.
[22]H. Jaqaman, A. Z. Mekjian, and L. Zamick, Phys. Rev. C **27**, 2782 (1983); **29**, 2067 (1984).
[23]W. Fowler, C. Engelbrecht, and S. Woosley, Astrophys. J. **226**, 984 (1978).
[24]A. Goodman, J. Kapusta, and A. Z. Mekjian, Phys. Rev. C **30**, 851 (1984).
[25]L. Csernai and J. Kapusta, Phys. Rep. **131**, 223 (1986).
[26]G. Bertsch and P. Siemens, Phys. Lett. **126B**, 9 (1983).
[27]C. Kittle and H. Kromer, *Thermal Physics* (Freeman, New York, 1980).
[28]S. Levit and P. Bonche, Nucl. Phys. **A437**, 426 (1985).
[29]P. Bonche, S. Levit, and D. Vautherin, Nucl. Phys. **A427**, 278 (1984).
[30]A. R. DeAngelis and A. Z. Mekjian, RU-88-59 (submitted to Phys. Rev. C).